Journal of Cranio-Maxillo-Facial Surgery 44 (2016) 202–209

Contents lists available at ScienceDirect

Journal of Cranio-Maxillo-Facial Surgery

journal homepage: www.jcmfs.com

Accuracy of open-source software segmentation and paper-based printed three-dimensional models

Piotr Szymor [a,*], Marcin Kozakiewicz [a], Raphael Olszewski [b]

[a] Department of Maxillofacial Surgery (Chair: Prof. M. Kozakiewicz DDS, PhD), Medical University of Lodz, Zeromskiego 113, 90-549 Lodz, Poland
[b] Oral and Maxillofacial Surgery Research Lab IREC/CHEX/OMFS (Chair: Prof. Raphael A. Olszewski DDS, MD, PhD), Université Catholique de Louvain, Av. Hippocrate, 55 – B1.55.04, B-1200 Brussels, Belgium

A R T I C L E I N F O

Article history:
Paper received 23 August 2015
Accepted 4 November 2015
Available online 14 November 2015

Keywords:
Anatomical models
CAD–CAM
Cone beam computed tomography
Maxillofacial surgery
Surgical models

A B S T R A C T

In this study, we aimed to verify the accuracy of models created with the help of open-source Slicer 3.6.3 software (Surgical Planning Lab, Harvard Medical School, Harvard University, Boston, MA, USA) and the Mcor Matrix 300 paper-based 3D printer. Our study focused on the accuracy of recreating the walls of the right orbit of a cadaveric skull.

Cone beam computed tomography (CBCT) of the skull was performed (0.25-mm pixel size, 0.5-mm slice thickness). Acquired DICOM data were imported into Slicer 3.6.3 software, where segmentation was performed. A virtual model was created and saved as an .STL file and imported into Netfabb Studio professional 4.9.5 software. Three different virtual models were created by cutting the original file along three different planes (coronal, sagittal, and axial). All models were printed with a Selective Deposition Lamination Technology Matrix 300 3D printer using 80 gsm A4 paper. The models were printed so that their cutting plane was parallel to the paper sheets creating the model. Each model (coronal, sagittal, and axial) consisted of three separate parts (~200 sheets of paper each) that were glued together to form a final model. The skull and created models were scanned with a three-dimensional (3D) optical scanner (Breuckmann smart SCAN) and were saved as .STL files. Comparisons of the orbital walls of the skull, the virtual model, and each of the three paper models were carried out with GOM Inspect 7.5SR1 software. Deviations measured between the models analysed were presented in the form of a colour-labelled map and covered with an evenly distributed network of points automatically generated by the software. An average of 804.43 ± 19.39 points for each measurement was created. Differences measured in each point were exported as a .csv file. The results were statistically analysed using Statistica 10, with statistical significance set at $p < 0.05$.

The average number of points created on models for each measurement was 804.43 ± 19.39; however, deviation in some of the generated points could not be calculated, and those points were excluded from further calculations. From 94% to 99% of the measured absolute deviations were <1 mm.

The mean absolute deviation between the skull and virtual model was 0.15 ± 0.11 mm, between the virtual and printed models was 0.15 ± 0.12 mm, and between the skull and printed models was 0.24 ± 0.21 mm.

Using the optical scanner and specialized inspection software for measurements of accuracy of the created parts is recommended, as it allows one not only to measure 2-dimensional distances between anatomical points but also to perform more clinically suitable comparisons of whole surfaces. However, it requires specialized software and a very accurate scanner in order to be useful. Threshold-based, manually corrected segmentation of orbital walls performed with 3D Slicer software is accurate enough to be used for creating a virtual model of the orbit. The accuracy of the paper-based Mcor Matrix 300 3D printer is comparable to those of other commonly used 3-dimensional printers and allows one to

* Corresponding author. Tel.: +48 42 639 36 98.
E-mail address: piotr.szymor@gmail.com (P. Szymor).

http://dx.doi.org/10.1016/j.jcms.2015.11.002

create precise anatomical models for clinical use. The method of dividing the model into smaller parts and sticking them together seems to be quite accurate, although we recommend it only for creating small, solid models with as few parts as possible to minimize shift associated with gluing.

1. Introduction

Anatomical reconstruction is currently one of the main concerns in maxillofacial surgery. It is especially important in the orbital wall trauma, where restoring the correct shape of the orbit can significantly reduce complications (Jazwiecka-Koscielniak and Kozakiewicz, 2014; Kozakiewicz and Szymor, 2013; Kozakiewicz, 2014; Kozakiewicz et al., 2013a,b). Nowadays we can restore pre-trauma anatomy with the aid of three-dimensional (3D) virtual images created from computed tomography data, as well as real solid models created with additive manufacturing. Although currently used models seem to be sufficiently accurate (Salmi et al., 2013), the relatively high costs of creating real 3D models limit common use of this technology. Therefore decided to verify the accuracy of models created with help of open-source Slicer 3.6.3 software (Surgical Planning Lab, Harvard Medical School, Harvard University, Boston, Machusetts, USA) and Mcor Matrix 300 paper-based 3D printer (Olszewski et al., 2014). Our study focused on the accuracy of recreating walls of the right orbit of cadaveric skull. Because of printer problems with flawlessly printing models thicker than 200 sheets of paper, we separated the orbital model into three blocks of around 200 sheets of paper each and 3D printed them separately. We applied this technique to evaluate the accuracy of models printed from separate pieces. We wanted to know whether stacking together separate parts would have important influence on the accuracy of the final full model and whether this approach could bypass the drawbacks of the Mcor 3D printer. We also wanted to know whether there was a significant difference between models separated and re-formed again along axial, coronal, or sagittal plane. Final models were compared with the original skull with the help of optical scanner and specialized engineering software.

2. Material and methods

After close examination, due to very good quality of preserved orbital walls, skull number 17 from the anatomical collection of Faculté de Médecine et Medicine Dentaire, Department of Anatomy (Prof B. Lengélé) UCL was selected for further analysis. Cone beam computed tomography (CBCT) (Accuitomo, Morita, Kyoto, Japan) (Primo et al., 2012) of the skull was performed with the following parameters: 140 × 100-mm field of view, 90 kV, 5 mA, Hifi mode, 0.25-mm pixel size, and 0.5-mm slice thickness. Acquired DICOM data were imported into Slicer 3.6.3 (Egger et al., 2012; Pieper et al., 2004) software (Surgical Planning Lab, Harvard Medical School, Harvard University, Boston, MA, USA). Then, automatic threshold-based segmentation was performed. Selected regions were manually corrected slice by slice in coronal view to completely close pseudo foramens present after automatic segmentation (Elgalal et al., 2010; Hohlweg-Majert et al., 2005; Kokemueller et al., 2008; Kozakiewicz et al., 2009; Metzger et al., 2007). The created virtual model (VM) was saved as an .STL file and imported into Netfabb Studio professional 4.9.5 software (Netfabb, Parsberg, Germany). Three different virtual models were created by cutting the original file along three different planes (coronal, sagittal, and axial) (Fig. 1). All created models were printed with a low-cost, paper-based Matrix 300 3D printer (Mcor Technologies, Dunleer, Ireland), which is based on Selective Deposition Lamination technology. The printer is controlled by a personal computer with SliceIt 4.7 software (Mcor Technologies, Dunleer, Ireland). In this software, each imported part is analysed and cut into 0.1-mm layers that are equal to the thickness of the utilised 80 gsm A4 sheet of paper (Plantin, Evere, Belgium). The prepared two-dimensional (2D) data were sent to the Matrix 300 printer, where a tungsten blade cut a sheet of paper layer by layer according to the medical imaging data. The layers were glued together with water-soluble adhesive (Mcor Technologies, Dunleer, Ireland) (Olszewski et al., 2014). Each model was placed in the printing software so that its cutting plane was parallel to the paper sheets creating the model. After printing, parts were cleaned from the excess material in a process called "weeding." Each model (coronal, sagittal, and axial) consisted of three separate parts (~200 sheets of paper each) that were glued together to form a final model. Freed parts were stuck together using Pelifix glue (Pelikan, Hannover, Germany) (Fig. 2). The skull and created models were scanned with Breuckmann smart SCAN (Breuckmann, Meersburg, Germany), a 3D optical scanner provided by Cadmech (Wrocław, Poland) and saved as .STL files. Accuracy declared by the manufacturer for that optical scanning was 40–50 μm. Therefore it was possible to compare orbital walls of the skull, virtual model, and each of three full paper models. Those comparisons were carried out in GOM Inspect 7.5SR1 software (GOM, Braunschweig, Germany) as follows: skull versus virtual model, virtual model versus printed model (coronal, sagittal, and axial), and finally skull versus printed model (coronal, sagittal, and axial). After importing a pair of files for comparison to GOM software, they had to be aligned. To do so, one of the models (usually the skull, as the virtual model was used only when the skull was not compared) had to be marked as nominal element and the compared one as an actual element. As a first step, the

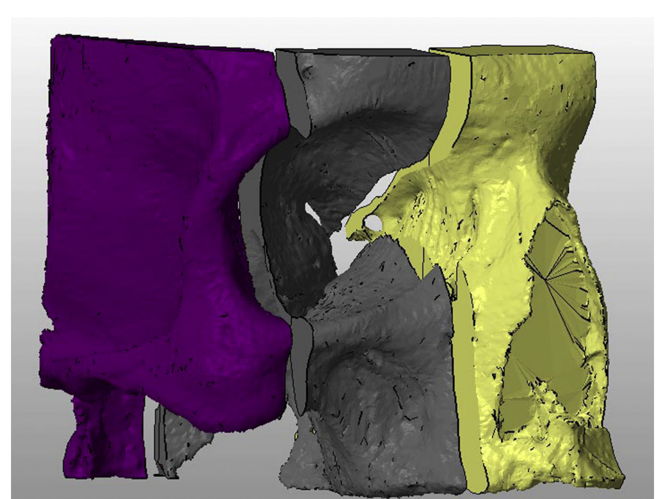

Fig. 1. Virtual model cut in the sagittal plane into three smaller parts. The .STL file created in the segmentation process was cut into smaller pieces along the coronal, sagittal, or axial plane to facilitate the printing process.

alignment was performed with a "prealignement" command, and later on, after selecting only orbital walls on both models, the final alignment was made with "local best fit" command. Alignment was checked and accepted by the author before further analysis was done. Next, deviations measured between analysed models were presented in the form of a colour-labelled map (Fig. 3) with the maximum distance for comparison set for 10 mm. On the created mesh orbital surface of each orbital wall was a manually selected set of evenly distributed network of points automatically generated by the software (Fig. 3). The distance between points was set to 2 mm, measured along the plane parallel to the selected area, because lower values resulted in a software error (too many points would be created). An average of 804.43 ± 19.39 points for each measurement were created. Differences measured at each point were exported as a .csv file. The results were statistically analysed using Statistica 10 (StatSoft Inc., Tulsa, OK, USA) with statistical significance set at $p < 0.05$.

3. Results

The average number of points created on models for each measurement was 804.43 ± 19.39 (Table 1). There were an average of 258 ± 13.47 points on the superior orbital wall, 218.14 ± 11.32 on the lateral wall, 153.57 ± 10.88 on the inferior wall, and 174.71 ± 14.45 on the medial orbital wall. However, the deviation in some of generated points could not be calculated (Table 1). Those points were excluded from further calculations. On average there were 8.43 ± 6.21 such points for each measurement. Most frequently they occurred on the medial (3.43 ± 3.95) and lateral (3.29 ± 2.50) walls. There were 1.57 ± 1.51 points without calculated deviations on the inferior orbital wall and only 0.14 ± 0.38 on the superior orbital wall. Most of those points, as well as points with large deviations when compared to the median, were located in or near the natural foramina of the orbit, i.e., the anterior and posterior ethmoidal foramina, lacrimal groove and nasolacrimal canal, and inferior and superior orbital fissure. In these areas, the point deviation between measured objects reached extreme values, as can be seen in Table 1. However, from 94% to 99% of measured absolute deviations were smaller than 1 mm. Therefore the Grubbs two-sided test with $p = 0.05$ was performed to eliminate such outliers for each orbital wall in each measurement separately. Test was re-run until there were no outliers left in the data used. There were usually 24 ± 12.74 points discarded in this way from further analysis for each measurement (Table 1).

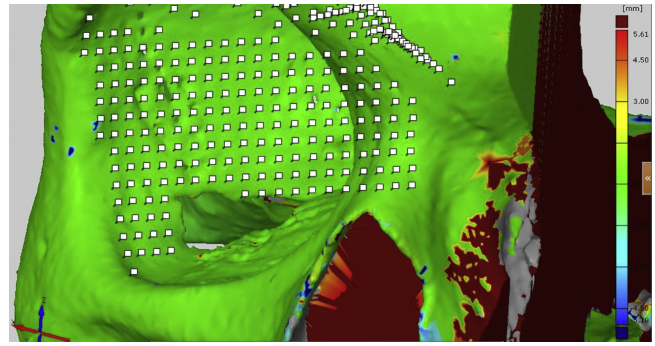

Fig. 3. Network of evenly distributed points on the surface of lateral and upper orbital walls. The network was created on a colour-labelled map of measured deviations between superimposed models. Distance between created points was set to 2 mm.

The mean absolute deviation between the skull and virtual model was 0.15 ± 0.11 mm (Table 1). Analysis of variance (ANOVA) showed that there was a statistically significant difference in absolute deviation between the measured walls ($p < 0.01$) There was no such difference between the medial and inferior wall ($p = 0.22$) (Table 2).

The mean absolute deviation between the virtual and printed models was 0.15 ± 0.12 mm. For the model cut in the axial plane, it was 0.13 ± 0.09 mm; for the model cut in the coronal plane 0.11 ± 0.07 mm, and for the model cut sagittally it was 0.22 ± 0.16 mm. ANOVA showed that there was statistically significant difference in measurements of absolute deviation between printed models and a virtual model for all printed models ($p < 0.01$). The sagittally cut model was different from the other models ($p < 0.01$). The difference between the models cut in the axial and coronal planes was also statistically significant ($p = 0.02$). Closer analysis (Table 3) showed that the differences between measurements on the superior, medial, and orbital walls for axially and coronally cut models were not statistically different ($p = 1.00$ and $p = 0.65$ for the lateral orbital wall). The only statistically significant difference was in measurements done on the inferior orbital wall ($p < 0.01$). The model cut in the sagittal plane had measurements of absolute deviation that were statistically significantly different from those of other models for each orbital wall ($p < 0.01$).

The mean absolute deviation between the skull and printed models was 0.24 ± 0.21 mm. Although the measured mean absolute

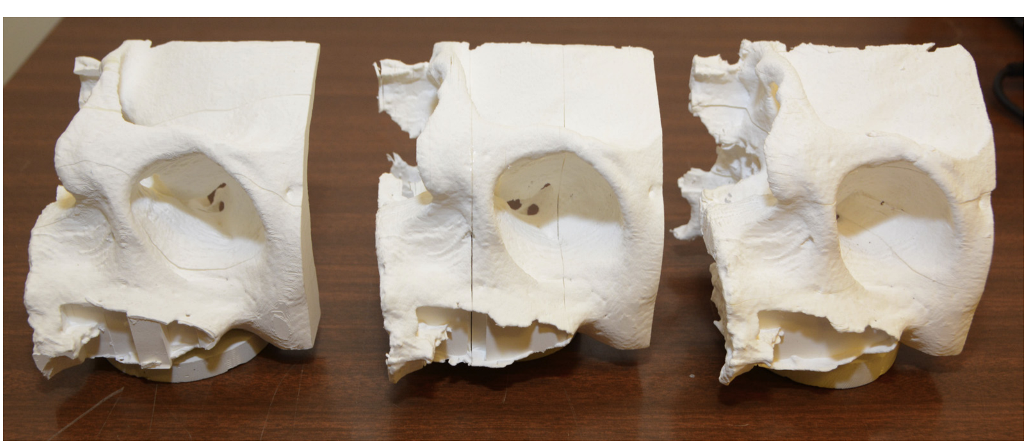

Fig. 2. Paper-based models printed on a Matrix 300 3D printer. Each model consists of three smaller parts, which were printed separately and later stuck together with glue. From the left, the models are cut in the coronal, axial, and sagittal planes.

Table 1
Measurement results.

Measurement/wall	Points created	Points without calculated deviation	Outlier points	Points measured	Mean deviation [mm]	Deviation SD [mm]	Minimal deviation [mm]	Maximal deviation [mm]	Mean absolute deviation [mm]	Absolute deviation SD [mm]
Skull vs virtual model	832	17	23	792	−0.05	0.18	−8.16	6.96	0.15	0.11
Superior	269	1	0	268	−0.03	0.11	−0.31	0.30	0.10	0.06
Lateral	223	2	4	217	−0.01	0.18	−4.04	6.96	0.14	0.11
Inferior	156	3	5	148	−0.17	0.18	−2.05	5.16	0.22	0.12
Medial	184	11	14	159	−0.04	0.23	−8.16	3.24	0.19	0.13
Axial vs virtual model	806	5	21	780	−0.09	0.13	−2.78	8.79	0.13	0.09
Superior	253	0	3	250	−0.08	0.12	−0.48	0.54	0.11	0.09
Lateral	217	4	4	209	−0.04	0.13	−0.43	8.79	0.10	0.09
Inferior	164	0	7	157	−0.17	0.12	−0.51	5.61	0.18	0.10
Medial	172	1	7	164	−0.10	0.13	−2.78	6.27	0.13	0.09
Coronal vs virtual model	798	11	37	750	−0.02	0.13	−7.49	9.40	0.11	0.07
Superior	255	0	11	244	−0.08	0.10	−7.49	2.98	0.11	0.07
Lateral	197	3	7	187	0.03	0.12	−4.02	9.40	0.10	0.07
Inferior	147	3	8	136	−0.04	0.11	−0.42	5.97	0.10	0.06
Medial	199	5	11	183	0.01	0.14	−2.70	7.83	0.13	0.07
Sagittal vs virtual model	827	13	43	771	−0.06	0.26	−7.31	8.46	0.22	0.16
Superior	272	0	8	264	0.03	0.23	−7.31	1.21	0.18	0.14
Lateral	221	8	13	200	−0.15	0.31	−6.48	0.80	0.28	0.20
Inferior	162	3	10	149	0.10	0.14	−6.45	8.46	0.15	0.09
Medial	172	2	12	158	−0.25	0.19	−0.60	6.42	0.28	0.14
Skull vs axial	780	2	7	771	0.02	0.24	−0.72	8.87	0.20	0.14
Superior	242	0	0	242	−0.22	0.18	−0.72	0.29	0.24	0.15
Lateral	218	2	2	214	0.09	0.17	−0.48	0.81	0.14	0.13
Inferior	152	0	3	149	0.26	0.12	−0.22	8.87	0.26	0.11
Medial	168	0	2	166	0.06	0.18	−0.34	0.75	0.15	0.11
Skull vs coronal	786	11	12	763	0.03	0.23	−3.58	5.93	0.18	0.14
Superior	242	0	2	240	−0.02	0.13	−3.58	1.17	0.10	0.08
Lateral	235	4	6	225	0.26	0.12	−2.30	5.93	0.27	0.12
Inferior	133	2	2	129	−0.01	0.19	−0.65	3.26	0.14	0.13
Medial	176	5	2	169	−0.17	0.20	−0.67	5.92	0.20	0.16
Skull vs sagittal	802	0	25	777	−0.24	0.38	−4.76	4.78	0.35	0.28
Superior	273	0	3	270	−0.22	0.31	−0.85	2.42	0.32	0.21
Lateral	216	0	4	212	−0.07	0.25	−1.55	4.78	0.22	0.15
Inferior	161	0	7	154	−0.09	0.31	−4.76	3.31	0.26	0.19
Medial	152	0	11	141	−0.71	0.33	−2.76	3.98	0.72	0.29

deviations for axially (0.20 ± 0.14 mm) and coronally (0.18 ± 0.14 mm) cut models were similar, there was a statistically significant difference between those measurements ($p = 0.01$). The mean absolute deviation in comparison of the skull and sagittally cut model was 0.35 ± 0.28 mm. ANOVA showed that there was a statistically significant difference for all three printed models ($p < 0.01$).

When comparing deviations measured on each orbital wall of the skull versus the printed model measurements, there was no statistically significant difference between the axially and coronally cut model only on medial orbital wall ($p = 0.09$). On the other orbital walls, such differences were statistically significant ($p < 0.01$). Surprisingly, the difference between measurements done in the sagittally and axial cut models on the inferior orbital wall was not statistically significant ($p = 0.17$). However, in comparisons of the skull versus the printed model, for the sagittally cut model the mean absolute deviation measured on the inferior wall (0.26 ± 0.19 mm) was one of the lowest, whereas for the axially cut model the mean absolute deviations on the inferior wall (0.26 ± 0.11 mm) were the greatest. Therefore, such lack of a statistically significant difference in this case should be considered as incidental.

For each case of measurements, a statistical analysis of measured absolute deviation differences between orbital walls was also performed (Table 2). In each of analysed superimpositions, ANOVA revealed a statistically significant difference between the measured absolute deviations on each orbital wall ($p < 0.01$).

4. Discussion

Although rapid prototyping techniques such as 3D printing and Computerized Numerical Control milling are commonly used in maxillofacial surgery (Jazwiecka-Koscielniak and Kozakiewicz, 2014; Kozakiewicz and Szymor, 2013; Kozakiewicz et al., 2013a,b), verification of the accuracy of the machines used has usually been done in 2D manner, by simple comparison of linear measurements between selected points (Choi et al., 2002; Ibrahim et al., 2009; Olszewski et al., 2014; Salmi et al., 2013; Silva et al., 2008). There are only a few articles indexed in PubMed in which authors verified the accuracy of additive manufactured models of bones created from previously acquired CT-derived DICOM data by using 3D scans (Anstey et al., 2011; Huotilainen et al., 2014; Pan et al., 2014). Only one of those studies concerned the maxillofacial region (Huotilainen et al., 2014). Also, there are some studies verifying the accuracy of created 3D models from segmentation of hard tissues from DICOM files by comparing them with 3D scans of real objects (Akyalcin et al., 2013; Engelbrecht et al., 2013; Fourie et al., 2012; Martorelli et al., 2014; Shahbazian et al., 2010). The overall accuracy of 3D printed models is based on the sum of the errors made during the process of preparing and printing the parts.

Table 2
Statistical analysis of differences in absolute deviations between orbital walls.

Measurement	Wall	Lateral	Superior	Inferior	Medial
Skull vs virtual model	Lateral		<0.01	<0.01	<0.01
	Superior	<0.01		<0.01	<0.01
	Inferior	<0.01	<0.01		**0.22**
	Medial	<0.01	<0.01	**0.22**	
Axial vs virtual model	Lateral		**0.35**	<0.01	<0.01
	Superior	**0.35**		<0.01	**0.12**
	Inferior	<0.01	<0.01		<0.01
	Medial	<0.01	**0.12**	<0.01	
Coronal vs virtual model	Lateral		**1.00**	**1.00**	<0.01
	Superior	**1.00**		**1.00**	0.01
	Inferior	**1.00**	**1.00**		0.02
	Medial	<0.01	0.01	0.02	
Sagittal vs virtual model	Lateral		<0.01	<0.01	**0.86**
	Superior	<0.01		**1.00**	<0.01
	Inferior	<0.01	**1.00**		<0.01
	Medial	**0.86**	<0.01	<0.01	
Skull vs axial	Lateral		<0.01	<0.01	**1.00**
	Superior	<0.01		**0.06**	<0.01
	Inferior	<0.01	**0.06**		<0.01
	Medial	**1.00**	<0.01	<0.01	
Skull vs coronal	Lateral		<0.01	<0.01	<0.01
	Superior	<0.01		0.03	<0.01
	Inferior	<0.01	0.03		<0.01
	Medial	<0.01	<0.01	<0.01	
Skull vs sagittal	Lateral		<0.01	**0.27**	<0.01
	Superior	<0.01		**0.12**	<0.01
	Inferior	**0.27**	**0.12**		<0.01
	Medial	<0.01	<0.01	<0.01	

For each superimposition of scanned models analysed, absolute deviations on each orbital wall were measured and compared with each other. The p value of ANOVA for between-wall comparisons is presented. Pairs of orbital walls, in which difference between measured absolute deviations was not statistically significant ($p < 0.05$), are given in boldface type.

Table 3
Statistical analysis of measured differences in absolute deviations between orbital virtual model and printed model for each orbital wall.

Wall	Measurement	Axial vs virtual model	Coronal vs virtual model	Sagittal vs virtual model
Lateral	Axial vs virtual model		**0.65**	<0.01
	Coronal vs virtual model	**0.65**		<0.01
	Sagittal vs virtual model	<0.01	<0.01	
Superior	Axial vs virtual model		**1.00**	<0.01
	Coronal vs virtual model	**1.00**		<0.01
	Sagittal vs virtual model	<0.01	<0.01	
Inferior	Axial vs virtual model		<0.01	0.01
	Coronal vs virtual model	<0.01		<0.01
	Sagittal vs virtual model	0.01	<0.01	
Medial	Axial vs virtual model		**1.00**	<0.01
	Coronal vs virtual model	**1.00**		<0.01
	Sagittal vs virtual model	<0.01	<0.01	

For each superimposition of printed models analysed and virtual model, absolute deviations on each orbital wall were measured and compared with each other. The p value of ANOVA for between-superimpositions comparison is presented for each orbital wall separately. Pairs of superimpositions, in which the difference between measured absolute deviations was not statistically significant ($p < 0.05$), are given in boldface type.

Similar to other studies (Anstey et al., 2011; Engelbrecht et al., 2013; Fourie et al., 2012; Huotilainen et al., 2014; Martorelli et al., 2014; Moerenhout et al., 2009; Olszewski et al., 2008; Pan et al., 2014), we created our models with threshold segmentation. Unfortunately this process is not error-free (Engelbrecht et al., 2013; Fourie et al., 2012; Huotilainen et al., 2014). Manual correction performed thereafter focused mainly on closing pseudo foraminas generated in the threshold segmentation protocol. To do so, and also to facilitate further printing of the 3D model, paranasal sinuses (i.e., maxillary, frontal, and ethmoidal sinuses) were incorporated into the model. Manual segmentation was done slice by slice in the coronal view until the results were the authors deemed it satisfactory. Despite the small voxel size, using a cadaver skull without soft tissues, and with care taken in this process because of the nature of the DICOM data (Engelbrecht et al., 2013; Fourie et al., 2012; Huotilainen et al., 2014), it was impossible to precisely mark the bone margins (Fig. 4). This was clearly visible in or near the natural foramina of the orbit (i.e., the anterior and posterior ethmoidal foramina, lacrimal groove and nasolacrimal canal, and inferior and superior orbital fissure), because some of these foramina were unintentionally made smaller or even closed during manual segmentation. This was associated with the occurrence of extreme deviations in such places, and such values as clear outliers had to be discarded. Although accuracy of segmentation is associated with voxel size (Martorelli et al., 2014), there is no significant difference whether CT or CBCT is used (Martorelli et al., 2014; Olszewski et al., 2008). In this study, we used CBCT with a 0.25-mm pixel size and a 0.5-mm slice thickness.

Therefore, the accuracy of segmentation is the first factor that influences the overall accuracy of printed models. Nevertheless, the results of this study show very good accuracy of hard tissue segmentation with 3D Slicer software. The mean deviation between the skull and the virtual model was only -0.05 ± 0.18 mm, and the average absolute deviation was 0.15 ± 0.11 mm. The values acquired are similar to those found in other studies (Table 4).

The other factor that has a great influence on the accuracy of printed models is the actual accuracy of the printer used (Salmi et al., 2013). In this study, the overall mean accuracy of printed models compared with virtual models was 0.15 ± 0.12 mm. This result is comparable to those of other studies (Table 5).

Another factor that is important in planning such a study is the accuracy of the measuring tool used, because it can also influence the final results. In this study, we used 3D models created with a Breuckmann smart SCAN (Breuckmann, Meersburg, Germany) 3D optical scanner. The optical scanner requires an unobstructed field of view for the camera in order to scan the object successfully (Huotilainen et al., 2014). This issue is resolved by rotating the physical object and creating the virtual object with overlap of the earlier scanned parts in specialized software. Therefore, after a few unsuccessful attempts at scanning with optical and laser scanners available at the Medical University of Lodz, we decided to subcontract Cadmech (Wrocław, Poland) to perform the scanning. The accuracy of scanning was 40–50 μm and greatly surpassed the accuracy of CBCT; therefore it should not have a significant influence on the results obtained.

Furthermore, some details were lost in the “weeding” process. During this process, freeing large and rather flat surfaces usually is problem-free; however, small and protruding elements are usually lost. Sometimes freeing excess material located in or nearby natural foramina of the orbit, i.e., the anterior and posterior ethmoidal foramina, lacrimal groove and nasolacrimal canal, and inferior and superior orbital fissure has been very difficult, if not impossible, without damaging nearby structures (Kozakiewicz et al., 2013a,b). Moreover, in such areas, segmentation from CBCT DICOM files also was done manually and is prone to errors (Engelbrecht et al., 2013; Fourie et al., 2012; Moerenhout et al., 2009). The weeding process is also time consuming. For models presented in this study, the weeding process took one investigator 17 h 10 min for the sagittal model, 13 h 20 min for the coronal model, and 10 h 35 min for the axial model. The models were freed in the above order.

Another factor that also influenced the overall accuracy of the created models was the fact that each model was actually made from three separate parts that had to be stuck together. A 3D printer Mcor Matrix 300 has some disadvantages in terms of production

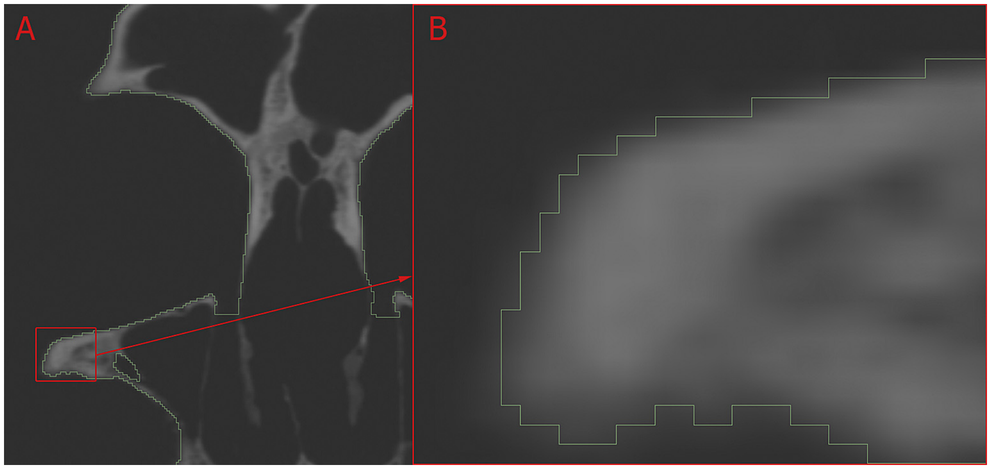

Fig. 4. Segmentation in 3D Slicer. Visible jagged edge of selection in magnification.

Table 4
Accuracy of segmentation in different studies.

Author	Anatomy compared	Method of comparison	Software used for segmentation	Absolute mean [mm]	Mean [mm]	Max [mm]
Anstey et al. (Anstey et al., 2011)	VM vs SC Proximal femur	Models superimposition	Mimics	0.58 ± 0.61	−0.48	1.62
Anstey et al. (Anstey et al., 2011)	VM vs SC Acetabulum	Models superimposition	Mimics	0.72 ± 0.81	−0.59	2.86
Engelbrecht et al. (Engelbrecht et al., 2013)	VM vs SC Human mandible	Linear measurements	SimPlant Ortho Pro			1.98 ± 1.37 2.15 ± 1.30
Fourie et al. (Fourie et al., 2012)	VM vs SC Human mandible	Models superimposition	SimPlant Ortho Pro		0.330 ± 0.427 0.763 ± 0.392	
Huotilainen et al. (Huotilainen et al., 2014)	SP vs SP Human skull	Models superimposition	Mango 3D Slicer STL Model Creator Planmeca ProModel			>1 mm
Martorelli et al. (Martorelli et al., 2014)	VM vs SM	Models superimposition	Scanora 3D		0.137 ± 0.159	1.365
Shahbazian et al. (Shahbazian et al., 2010)	VM vs SP Wisdom tooth	Models superimposition	Scanora		80% between −0.25 and 0.25	2.1–2.5
Akyalcin et al. (Akyalcin et al., 2013)	VM vs SM Teeth arch	Linear measurements	Anatomage		0.32 ± 0.06	
Richard et al. (Richard et al., 2014)	VM vs C	Linear measurements			0.25 ± 2.07	3.04
Choi et al.(Choi et al., 2002)	VM vs C Skull	Linear measurements	V-Works	0.49 ± 0.34		1.08
Present study	VM vs SC Skull	Models superimposition	3D Slicer 3.6.3	0.15 ± 0.11	−0.05 ± 0.18	0.75

VM = virtual model generated from DICOM data; SC = scanned cadaver; SB = scanned benchmark model; SP = scanned printed model; C = cadaver; P = printed model.

Table 5
Comparison of virtual and printed models in different studies.

Author	Anatomy compared	Method of comparison	Technology for creating model	Absolute mean [mm]	Mean [mm]	Max [mm]
Anstey et al.(Anstey et al., 2011)	VM vs SP Proximal femur	Models superimposition	FDM	0.47 ± 0.49	−0.46	0.94
Anstey et al.(Anstey et al., 2011)	VM vs SP Acetabulum	Models superimposition	FDM	0.55 ± 0.58	−0.55	1.91
Salmi et al.(Salmi et al., 2013)	VM vs P	Point inspection	SLS	0.93 ± 0.38–0.41		1.89
Salmi et al.(Salmi et al., 2013)	VM vs P	Point inspection	3DP	0.44–0.80 ± 0.25–0.51		1.66
Salmi et al.(Salmi et al., 2013)	VM vs P	Point inspection	PolyJet	0.20 ± 0.14		0.49
Choi et al.(Choi et al., 2002)	C vs P Skull	Linear measurements	SLA	0.57 ± 0.62		2.23
Present study	VM vs SP Czaszka	Nałożenie brył	SDL	0.13 ± 0.09 0.11 ± 0.07 0.22 ± 0.16	−0.09 ± 0.13 −0.02 ± 0.13 −0.06 ± 0.26	1.17

VM = virtual model generated from DICOM data; SC = scanned cadaver; SB = scanned benchmark model; SP = scanned printed model; C = cadaver; P = printed model; FDM = fused deposition modelling; SLA = stereolithography; SDL = selective deposition lamination; 3DP = 3D printing; SLS = selective laser sintering.

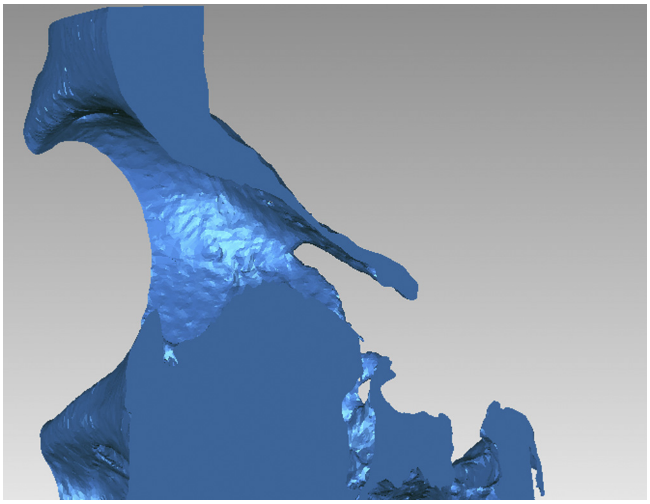

Fig. 5. View of a connection between the middle and lateral part of a model cut in the sagittal plane. The thin part of the model creating the superior orbital wall is visible.

time: the 3D printing of the orbit model used in our experiment took 24 h, with 8 h used for each pack of approximately 200 sheets of paper, and a 1-km run of the tungsten blade for the orbit. There was a need for a specific type of paper (not all types of A4 format paper are capable of being used in the 3D Mcor printer, as is stated in the Mcor technical instructions); and a paper jam frequently occurs if the room temperature and humidity are not controlled, resulting in frequent stops and errors during the entire process. From our own experience, these problems seem to be more frequent if a full model is made of more than 200 sheets of paper.

Therefore, some of those models were more accurate than others. The least precise model was that cut in the sagittal plane. The mean absolute deviation on that model was clearly greater than those measured on other two models, for comparisons of both the virtual model versus the printed model and the skull versus the printed model. Such differences may be caused by several factor. One is the flexibility of the printed paper model. The sagittally cut model was more vulnerable to such deformation than the other models because it is quite large, still thin, and almost without supported elements, such as a superior orbital wall in the middle part (Fig. 5). Furthermore, the cutting plane was also the plane in which paper layers creating the object were placed. In the sagittally oriented model, the weeding process was more complicated and took more than 17 h. However, this may be associated with the fact that the model cut in the sagittal plane was the first model printed, freed, and stuck together for the purpose of this study. This also may be the reason why this model is less accurate than the others.

The influence of cutting the model into smaller parts, which were later stuck together, can be seen in the mean deviation values measured for each orbital wall. Comparison between different printed models and the virtual model shows that the orbital walls parallel to the cutting plane are slightly less accurate than the walls perpendicular to the cutting plane. This is clearly visible in the sagittally and axially cut models (Table 1), where the lateral and medial orbital wall in the sagittally cut model or the inferior orbital wall in the axially cut model are shifted slightly more than the other walls. There seems to be no such correlation in the coronally cut model, because all orbital walls are virtually perpendicular to the cutting plane in this model. An ANOVA comparison (Table 2) seems to confirm such a statement, although the measured differences are very small.

All of the above-mentioned factors contribute to the overall accuracy of the 3D printer used when comparing the printed model to the actual skull. Similar methods to that used in this study, i.e., comparison of scans of actual bone and its 3D printed model created from CT or CBCT data, was found in only a few other articles (Anstey et al., 2011; Pan et al., 2014). However, there are many articles about the accuracy of printed models (Table 6), in which

Table 6
Comparison of bone and printed model in different studies.

Author	Anatomy compared	Method of comparison	Technology for creating model	Absolute mean [mm]	Mean [mm]	Max [mm]
Anstey et al. (Anstey et al., 2011)	SC vs SP Proximal femur	Models superimposition	FDM	0.42 ± 0.48	−0.32	1.58
Anstey et al. (Anstey et al., 2011)	SC vs SP Acetabulum	Models superimposition	FDM	0.47 ± 0.54	−0.43	1.94
Pan et al. (Pan et al., 2014)	SC vs SP Canine rib	Models superimposition	SLA		0.253 ± 0.346	2.126
Olszewski et al. (Olszewski et al., 2014)	C vs P Mandible	Linear measurements	SDL	0.36 ± 0.29		1.67
Choi et al. (Choi et al., 2002)	C vs P Skull	Linear measurements	SLA	0.62 ± 0.35		1.15
Taft et al. (Taft et al., 2011)	C vs P Skull	Linear measurements	SLA	0.608 ± 0.096		0.703
Nizam et al. (Nizam et al., 2006)	C vs P Skull	Linear measurements	SLA	0.23 ± 1.37		
Silva et al. (Silva et al., 2008)	C vs P Skull	Linear measurements	3DP		1.07	
Silva et al.(Silva et al., 2008)	C vs P Skull	Linear measurements	SLS		0.89	
Ibrahim et al. (Ibrahim et al., 2009)	C vs P Mandible	Linear measurements	SLS		0.90	2.52
Ibrahim et al. (Ibrahim et al., 2009)	C vs P Mandible	Linear measurements	3DP		1.44	3.19
Ibrahim et al. (Ibrahim et al., 2009)	C vs P Mandible	Linear measurements	PolyJet		1.23	3.92
Present study	VM vs SP Skull	Models superimposition	SDL	0.20 ± 0.14 0.18 ± 0.14 0.35 ± 0.28	0.02 ± 0.24 0.03 ± 0.23 −0.24 ± 0.38	1.3

VM = virtual model generated from DICOM data; SC = scanned cadaver; SB = scanned benchmark model; SP = scanned printed model; C = cadaver; P = printed model; FDM = fused deposition modelling; SLA = stereolithography; SDL = selective deposition lamination; 3DP = 3D printing; SLS = selective laser sintering.

comparison is done by linear measurements on the actual skull and printed model. Results gathered in this study show good accuracy of the used for creating printed models, comparable to other commonly used methods (Table 6).

5. Conclusions

Use of the optical scanner and specialized inspection software for measurements of the accuracy of created parts is recommended, as it allows one not only to measure 2D distances between anatomical points but also to perform a more clinically relevant comparison of whole surfaces. However, it requires specialized software and a very accurate scanner to be useful. Threshold-based, manually corrected segmentation of orbital walls performed with 3D Slicer software is accurate enough to be used for creating a virtual model of the orbit. The accuracy of the paper-based Mcor Matrix 300 3D printer is comparable to that of other commonly used 3D printers and allows one to create precise anatomical models for clinical purposes. The method of dividing the model into smaller parts and sticking them together seems to be quite accurate, although we recommend it only for creating small, solid models with as few parts as possible to minimize shifts associated with gluing.

Financial support

This study was supported by Medical University of Lodz, grant no 503/5-061-02/503-01, and by a grant for young researchers from the Marshal Office of the Lodz Voivodeship in Poland.

Conflict of interest

None declared.

Acknowledgements

We would like to thank the Fondation Saint Luc-Fonds Hervé Reychler 2013, Cliniques Universitaires Saint Luc, Brussels, Belgium, for a grant that allowed Pr Raphael Olszewski to purchase an Mcor Matrix 300 three-dimensional printer for the OMFS Lab (SSS/IREC/CHEX).

References

Akyalcin S, Dyer DJ, English JD, Sar C: Comparison of 3-dimensional dental models from different sources: diagnostic accuracy and surface registration analysis. Am J Orthod Dentofacial Orthop 144: 831–837, 2013
Anstey JB, Smith EJ, Rasquinha B, Rudan JF, Ellis RE: On the use of laser scans to validate reverse engineering of bony anatomy. Stud Health Technol Inform 163: 18–24, 2011
Choi JY, Choi JH, Kim NK, Kim Y, Lee JK, Kim MK, et al: Analysis of errors in medical rapid prototyping models. Int J Oral Maxillofac Surg 31: 23–32, 2002
Egger J, Kapur T, Nimsky C, Kikinis R: Pituitary adenoma volumetry with 3D slicer. PLoS One 7: e51788, 2012
Elgalal M, Kozakiewicz M, Loba P, Walkowiak B, Olszycki M, Stefańczyk L: Patient specific implants, designed using rapid prototyping and diagnostic imaging, for the repair of orbital fractures. Med Sci Monit 16: 75–79, 2010
Engelbrecht WP, Fourie Z, Damstra J, Gerrits PO, Ren Y: The influence of the segmentation process on 3D measurements from cone beam computed tomography-derived surface models. Clin Oral Investig 17: 1919–1927, 2013
Fourie Z, Damstra J, Schepers RH, Gerrits PO, Ren Y: Segmentation process significantly influences the accuracy of 3D surface models derived from cone beam computed tomography. Eur J Radiol 81: e524–e530, 2012
Hohlweg-Majert B, Schön R, Schmelzeisen R, Gellrich N-C, Schramm A: Navigational maxillofacial surgery using virtual models. World J Surg 29: 1530–1538, 2005
Huotilainen E, Jaanimets R, Valášek J, Marcián P, Salmi M, Tuomi J, et al: Inaccuracies in additive manufactured medical skull models caused by the DICOM to STL conversion process. J Craniomaxillofac Surg 42: 259–265, 2014
Ibrahim D, Broilo TL, Heitz C, de Oliveira MG, de Oliveira HW, Nobre SMW, et al: Dimensional error of selective laser sintering, three-dimensional printing, and PolyJet models in the reproduction of mandibular anatomy. J Craniomaxillofac Surg 37: 167–173, 2009
Jazwiecka-Koscielniak E, Kozakiewicz M: A new modification of the individually designed polymer implant visible in X-ray for orbital reconstruction. J Craniomaxillofac Surg 42: 1520–1529, 2014
Kokemueller H, Tavassol F, Ruecker M, Gellrich N-C: Complex midfacial reconstruction: a combined technique of computer-assisted surgery and microvascular tissue transfer. J Oral Maxillofac Surg 66: 2398–2406, 2008
Kozakiewicz M: Computer-aided orbital wall defects treatment by individual design ultrahigh molecular weight polyethylene implants. J Craniomaxillofac Surg 42: 283–289, 2014
Kozakiewicz M, Elgalal M, Loba P, Komuński P, Arkuszewski P, Broniarczyk-Loba A, et al: Clinical application of 3D pre-bent titanium implants for orbital floor fractures. J Craniomaxillofac Surg 37: 229–234, 2009
Kozakiewicz M, Elgalal M, Walkowiak B, Stefanczyk L: Technical concept of patient-specific, ultrahigh molecular weight polyethylene orbital wall implant. J Craniomaxillofac Surg 41: 282–290, 2013a
Kozakiewicz M, Szymor P: Comparison of pre-bent titanium mesh versus polyethylene implants in patient specific orbital reconstructions. Head Face Med 9: 32, 2013
Kozakiewicz M, Szymor P, Olszewski R: Three dimensional paper models experimental validation in vitro. Int J Oral Maxillofac Surg 42: 1256–1257, 2013b
Martorelli M, Ausiello P, Morrone R: A new method to assess the accuracy of a cone beam computed tomography scanner by using a non-contact reverse engineering technique. J Dent 42: 460–465, 2014
Metzger MC, Schön R, Tetzlaf R, Weyer N, Rafii A, Gellrich N-C, et al: Topographical CT-data analysis of the human orbital floor. Int J Oral Maxillofac Surg 36: 45–53, 2007
Moerenhout BAMML, Gelaude F, Swennen GRJ, Casselman JW, Van Der Sloten J, Mommaerts MY: Accuracy and repeatability of cone-beam computed tomography (CBCT) measurements used in the determination of facial indices in the laboratory setup. J Craniomaxillofac Surg 37: 18–23, 2009
Nizam A, Gopal RN, Naing L, Hakim AB, Samsudin AR: Dimensional accuracy of the skull models produced by rapid prototyping technology using stereolithography apparatus. Arch Orofac Sci 1: 60–66, 2006
Olszewski R, Reychler H, Cosnard G, Denis JM, Vynckier S, Zech F: Accuracy of three-dimensional (3D) craniofacial cephalometric landmarks on a low-dose 3D computed tomograph. Dentomaxillofac Radiol 37: 261–267, 2008
Olszewski R, Szymor P, Kozakiewicz M: Accuracy of three-dimensional, paper-based models generated using a low-cost, three-dimensional printer. J Craniomaxillofac Surg 42: 1847–1852, 2014
Pan Y, Zheng R, Liu F, Jing W, Yong C, Liang X, et al: The use of CT scan and stereo lithography apparatus technologies in a canine individualized rib prosthesis. Int J Surg 12: 71–75, 2014
Pieper S, Halle M, Kikinis R: 3D slicer. Biomed Imaging Nano Macro 2: 1–4, 2004
Primo BT, Presotto AC, de Oliveira HW, Gassen HT, Miguens SAQ, Silva AN, et al: Accuracy assessment of prototypes produced using multi-slice and cone-beam computed tomography. Int J Oral Maxillofac Surg 41: 1291–1295, 2012
Richard AH, Parks CL, Monson KL: Accuracy of standard craniometric measurements using multiple data formats. Forensic Sci Int 242C: 177–185, 2014
Salmi M, Paloheimo K-S, Tuomi J, Wolff J, Mäkitie A: Accuracy of medical models made by additive manufacturing (rapid manufacturing). J Craniomaxillofac Surg 41: 603–609, 2013
Shahbazian M, Jacobs R, Wyatt J, Willems G, Pattijn V, Dhoore E, et al: Accuracy and surgical feasibility of a CBCT-based stereolithographic surgical guide aiding autotransplantation of teeth: in vitro validation. J Oral Rehabil 37: 854–859, 2010
Silva DN, Gerhardt de Oliveira M, Meurer E, Meurer MI, Lopes da Silva JV, Santa-Bárbara A: Dimensional error in selective laser sintering and 3D-printing of models for craniomaxillary anatomy reconstruction. J Craniomaxillofac Surg 36: 443–449, 2008
Taft RM, Kondor S, Grant GT: Accuracy of rapid prototype models for head and neck reconstruction. J Prosthet Dent 106: 399–408, 2011